

ANALYSIS OF THE SYNCHROTRON RADIATION FROM SEGMENTED UNDULATOR IN DOUBLE-MINI BETA FUNCTION

H.W. Luo^{1,†}, T.Y. Chung², C.S. Hwang^{1,2,3}, C.H. Lee^{1,4}

¹ Graduate Program in Science & Technology of Synchrotron Light Source, National Tsing Hua University, Hsinchu, Taiwan

² National Synchrotron Radiation Research Center, Hsinchu, Taiwan

³ Department of Electrophysics, National Chiao Tung University, Hsinchu, Taiwan

⁴ Department of Engineering and System Science, National Tsing Hua University, Hsinchu, Taiwan

Abstract

Three long straight sections with double-mini beta-y lattice were created in the Taiwan Photon Source (TPS) for which the effects of focusing elements and phase shifters between the collinear undulators result in incorrect calculations of the brilliance while assuming a Gaussian-approximation. Therefore, an on-axis Wigner distribution function (WDF), which includes effects of wave phenomena, is a natural way to measure the intensity of synchrotron radiation and is used in this article as the definition of brilliance.

INTRODUCTION

To generate a high brilliant synchrotron radiation (SR), a large number of periods of an undulator and a low emittance of an electron beam are desired. A segmented undulator in a double mini beta-y lattice is implemented in TPS [1]. The SRs emitted by two undulator have a phase matching using a phase shifter [2]. A set of quadrupole magnets (QM) is inserted between two undulators to reduce the average vertical beta-function. In addition to reduce the emittance in the middle of an undulator, the method increases the electron beam lifetime especially operating at a small gap of in-vacuum undulators. Although the segmented undulator has advantages, a non-Gaussian distribution of SR, a dephasing concern for QMs and the drift space will increase a difficulty to evaluate the performance of SR, such as brilliance and coherent flux. In this article, we analyse such effects quantitatively through WDF.

EFFECT OF THE QUADRUPOLE MAGNET

The QMs change the trajectories of off-axis electrons (see fig. 2(a)) and cause a phase shift between the two radiation waves from both undulators generated by each electron. Since the phase differences are different for radiation from each electron, the profiles of the angular distribution are different (fig. 2(b)). The phase difference with respect to the radiation generated by an on-axis electron is

$$\Delta\phi = kc \frac{\Delta L}{\beta c}, \quad (1)$$

where k is the radiation wave number, c and βc is the speed of light and electron, respectively, and $\Delta L =$

[†] email address: luo.hw@nsrc.org.tw

$L_{off-axis} - L_{on-axis}$ is the path length difference of the electron in the region between the two undulators.

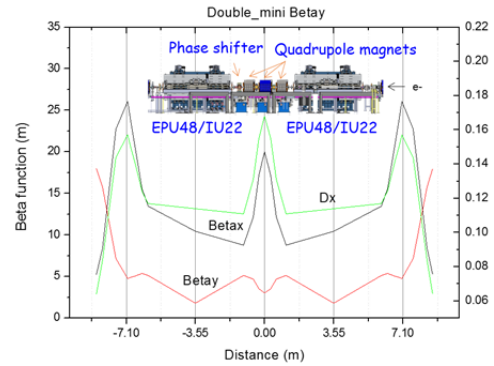


Figure 1: β function for a double mini- β_y lattice.[1,2].

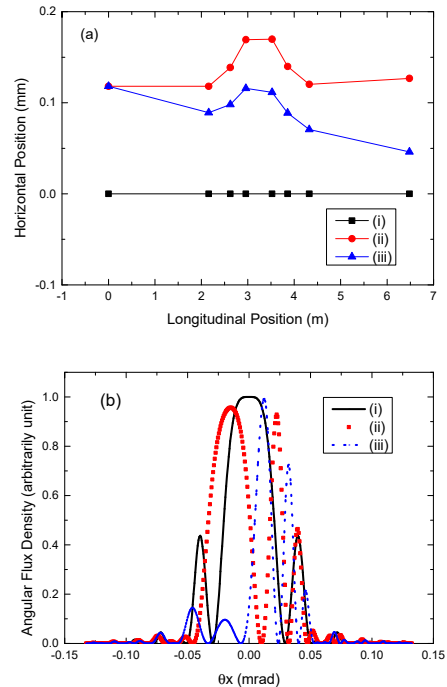


Figure 2: (a) Trajectories in the horizontal plane for electrons of different initial phase space coordinates (i)-(iii). (b) Profiles of the angular radiation distribution as generated by electrons travelling along trajectories corresponding to those in (a). The phase space coordinate (i) represent the on-axis electron and (ii), (iii) is the off-axis electron.

The phase difference depends on the wave number or the photon energy of the radiation and its coordinate distribution in phase space is different for different photon energies. For example, in the low energy region most of the radiation phase shift is less than 2π (as Fig. 3(a)), but could be several times 2π (Fig. 3(b)).

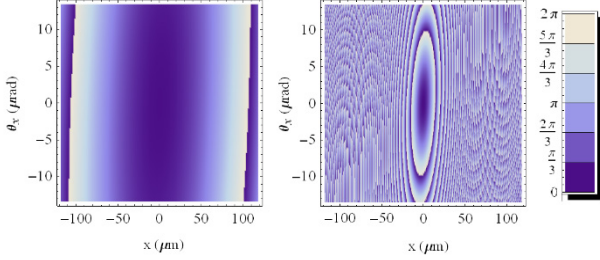


Figure 3: Distribution of radiation phase differences from electrons in different phase space positions for (a) 220 eV photons and (b) 12 keV photons. The scales in both position and angle are plus and minus one standard value of the electron beam size and divergence respectively.

EFFECT OF THE PHASE SHIFTER

A phase shifter is installed between the two undulators to adjust the radiation phase difference. The radiation profile strongly depends on the phase difference that is generated by the phase shifter. For instance, the profile of the radiation of a zero emittance electron beam is shown in Fig. 4.

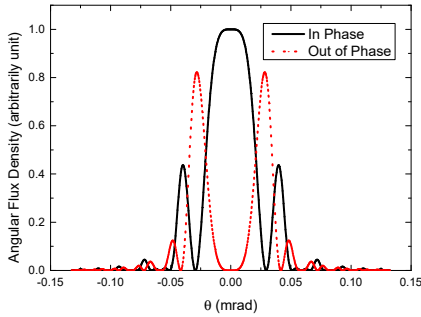


Figure 4: Radiation profile for a zero-emittance electron beam.

However, it should be noted that the maximum brilliance does not occur when the two radiation waves are completely in phase. The properties of the WDF results in the brilliance being directly related to the spectral flux of a symmetric radiation beam [3].

WIGNER DISTRIBUTION FUNCTION

The WDF was first introduced by Kim [4] as the definition of the synchrotron radiation brilliance and its properties and definitions have been reviewed by several other authors [3, 5, 6]. The brilliance can be defined by the WDF in different ways [3, 5]. Here, we choose the on-axis WDF as the brilliance definition, being in general the maximum value of the WDF for undulator radiation.

The mathematical form of the WDF and of the on-axis WDF are defined as follow,

$$W(\mathbf{r}, \boldsymbol{\theta}; \omega) = \left(\frac{1}{\lambda}\right)^2 \int \langle \mathcal{E}\left(\boldsymbol{\theta} - \frac{\boldsymbol{\theta}'}{2}; \omega\right) \mathcal{E}^*\left(\boldsymbol{\theta} - \frac{\boldsymbol{\theta}'}{2}; \omega\right) \rangle e^{ikr \cdot \boldsymbol{\theta}'} d^2 \boldsymbol{\theta}' \quad (2)$$

$$W_{on-axis} = W(\mathbf{0}, \mathbf{0}; \omega) = \left(\frac{1}{\lambda}\right)^2 \int \langle \mathcal{E}\left(\boldsymbol{\theta} - \frac{\boldsymbol{\theta}'}{2}; \omega\right) \mathcal{E}^*\left(\boldsymbol{\theta} - \frac{\boldsymbol{\theta}'}{2}; \omega\right) \rangle d^2 \boldsymbol{\theta}' \quad (3)$$

where $\mathbf{r} = (x, y)$ and $\boldsymbol{\theta} = (\theta_x, \theta_y)$ are the transverse positions and angles, respectively. The quantity \mathcal{E} is the angular representation of the electric field in the frequency domain and λ is the corresponding wavelength. In light sources, the electron bunch length is longer than the wavelength and the total WDF is the incoherent summation of the radiation WDF for each electrons (W_{se}).

$$W(\mathbf{r}, \boldsymbol{\theta}) = \sum_{N_e} W_{se}(\mathbf{r}, \boldsymbol{\theta}) \quad (4)$$

The electric field for the first harmonic undulator radiation is calculated by the following equation [7]

$$\mathcal{E}_k(\boldsymbol{\theta}; z = 0) = \frac{ek[JJ]L_u}{8\pi\epsilon_0\gamma c\lambda^2} e^{-inN_u \frac{k-k_r}{k_r}} \times \text{sinc}\left[\pi N_u \left(\frac{k_r}{2k_u} \boldsymbol{\theta}^2 + \frac{k-k_r}{k_r}\right)\right] \quad (5)$$

$$[JJ] = J_0\left(\frac{K^2}{4 + 2K^2}\right) - J_1\left(\frac{K^2}{4 + 2K^2}\right)$$

where k_r is the wave number at the resonant energy, N_u is the number of undulator periods and $k_r = 2\pi/\lambda_u$ defines the undulator period length λ_u . The paraxial equation of the electric field with nonzero initial coordinates (x_j, x'_j, t_j) is

$$\mathcal{E}_k(\boldsymbol{\theta}; z = 0) = e^{i\omega t_j} e^{ik\boldsymbol{\theta} \cdot \mathbf{x}_j} \mathcal{E}_k(\boldsymbol{\theta} - \mathbf{x}'_j; z = 0). \quad (6)$$

Expression (6) for the electric field can be expanded to higher odd harmonics if the undulator period number is high enough to keep the radiation profile in the shape of a sinc function and symmetric in the radial direction (Fig. 5).

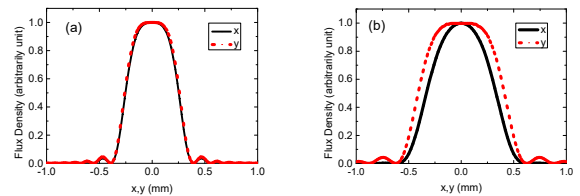


Figure 5: Radiation profile of the 5th harmonic of an IU22 in TPS (30 meters away from the source point) (a) for 140 periods, (b) for 20 periods.

To calculate the electric field for segmented undulators, the Fresnel diffraction formula [3]

$$\mathcal{E}_k(\boldsymbol{\theta}; z + l) = e^{ikl(1-\boldsymbol{\theta}^2/2)} \mathcal{E}_k(\boldsymbol{\theta}; z) \quad (7)$$

is used to combine the radiation field from all source points in each undulator to a common transverse plane wave (e.g. at the midpoint of both undulators).

$$\begin{aligned} \mathcal{E}_{segmented}(\theta; z = 0) &= e^{ik(L_u/2+d)(1-\theta^2/2)} \mathcal{E}_1(\theta; z = -L_u/2 - d) \\ &+ e^{i\omega\Delta t} e^{ik(-L_u/2-d)(1-\theta^2/2)} \mathcal{E}_2(\theta; z = L_u/2 + d) \quad (8) \\ \Delta t &= \frac{L_{12}}{\beta c} + \Delta t_{phase\ shifter} \end{aligned}$$

The path length of the electron from the first to the second virtual source plane be L_{12} and the initial conditions for \mathcal{E}_1 and \mathcal{E}_2 depend on the position and angle of the electron at the midpoint in each of the up- and down-stream undulators (Fig. 6).

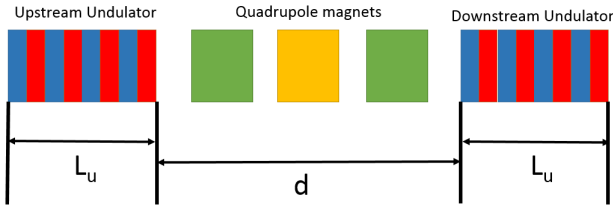


Figure 6: Arrangement of two collinear undulators used for the calculation of the radiation field.

COHERENT FLUX

We follow the procedure in the design report for the TPS beamline, where the coherent flux is calculated by integration of the photon flux through the coherent area as estimated by the van Cittert-Zernike theorem (the source size is the effective photon beam size in the middle of the downstream undulator) on the observer plane. In this article, the coherent area is the same for a segmented undulator. The overall degree of coherence is also calculated for comparison with the coherence property in this coherent area for single and double undulators. For an extended radiation source, the overall complex degree of coherence is obtained by the following equation [8]

$$\mu = \frac{\int I(x_1; z) I(x_2; z) \mu_{12}^2(x_1, x_2; z) dx_1 dx_2}{[\int I(r) dr]^2} \quad (9)$$

where μ_{12} is the complex degree of coherence for two points.

NUMERICAL RESULTS

The brilliance and coherent flux ratio for double and single undulators are calculated both for soft x-rays from 220 to 1600 eV and for hard x-ray from 9 to 12 keV to see whether double undulators can generate more brilliant light and provide more coherent flux compared to only one undulator.

The phase shifter plays an important role in the soft x-ray but not in the hard x-ray region as shown in Fig. 7. The brilliance could vary by several factors in the soft x-ray

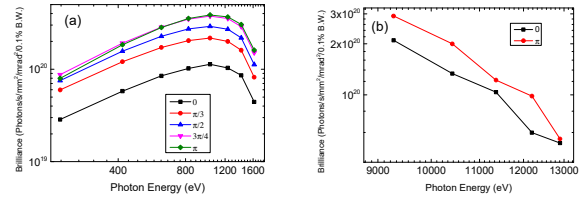


Figure 7: The effect of a phase shift in (a) the soft x-ray region and (b) the hard x-ray region.

region but only by about tens of percent in the hard x-ray region. This is because the interference effect of the two undulator radiation waves is clear in the soft x-ray region but not in the hard x-ray region.

The brilliance of single and double undulators is shown in Fig. 8. The ratio of the double to single undulator brilliance is about three in the soft x-ray region and 2.5 in the hard x-ray region. On the other hand, the ratio of coherent flux is about 2.1 at 220 eV but only 1.8 at 1.6 keV and 9 keV. The ratio of 1.8 is just the result of incoherent summation of the flux from two undulators. The overall degree of coherence for both single and double undulators is almost the same since the second source (upstream undulator) is farther away than the first source (downstream undulator). It should be noted that the phase of the phase shifter is π and 0 for the maximum value of brilliance and coherent flux, respectively.

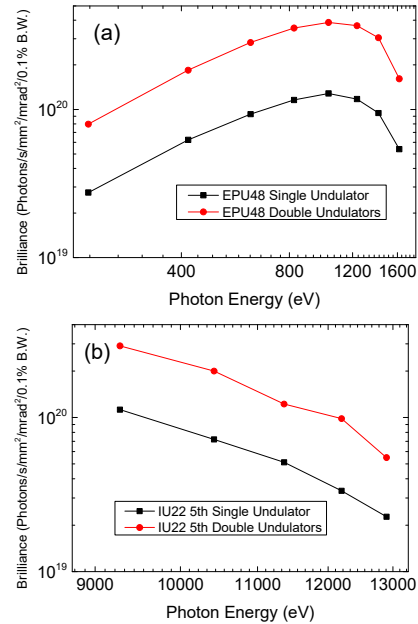


Figure 8: The brilliance for single and double undulators in (a) the soft x-ray region and (b) the hard x-ray region.

CONCLUSION

Using the on-axis WDF as the brilliance definition, we directly calculate the brilliance and measure the intensity of this type of light source and found that both brilliance and coherent flux can be enhanced by a second collinear undulator. Although the brilliance of segmented

undulators with a set of QM cannot be calculated analytically by Gaussian approximation.

REFERENCES

- [1] M.S. Chiu *et al.*, “Double Mini-Betay Optics for TPS Storage Ring”, *Proceedings of IPAC2010*, Kyoto, Japan, 2010, paper THPE030.
- [2] T.Y. Chung *et al.*, NIMA, 850, 72, 2017.
- [3] I.V. Bazarov, “Phys. Rev. Spec. Top. AB”, 15, 050703, 2012.
- [4] K.J. Kim, “Report No. LBL-20181”, 1985.
- [5] G. Geloni *et al.*, “J. Synchrotron Rad”, 22, 288, 2015
- [6] K.J. Kim, AIP Conference Proceedings, 184, 565, 1989.
- [7] R.R. Lindberg and K. J. Kim, “Phys. Rev. Spec. Top. AB”, 18, 090702, 2015.
- [8] A. Luis, J. Eur, “Opt. Soc.-Rapid”, 2 07030, 2007.